

Spiral instabilities in N-body simulations

J. A. Sellwood

University of Manchester

Abstract *N*-body simulations of disc galaxies that display recurrent transient spiral patterns are comparatively easy to construct, but are harder to understand. In this paper, I summarise the evidence from such experiments that the spiral patterns result from a recurrent spiral instability cycle. Each wave starts as rapidly growing, small-amplitude instability caused by a deficiency of particles at a particular angular momentum. The resulting large-amplitude wave creates, through resonant scattering, the conditions needed to precipitate a new instability.

1 Plan

The problem of spiral structure in galaxies has been worked on for many years but progress has been painfully slow. Most effort has been directed towards the development of an analytical (or at least semi-analytical) approach and many aspects of the problem have been discovered (see Sellwood 1989 for a review). Here, I collect the evidence from *N*-body simulations which indicates that the structure is continuously variable and results from a recurrent cycle of spiral instabilities.

A subsidiary purpose of this paper, is to convince the reader of the advantages of using *N*-body simulations *in tandem* with approximate analytic treatments. Without a close comparison of this nature, each separate approach is much less powerful; the limitations of the *N*-body experiments remain unquantified and the validity of the approximations in the analytic approach cannot be assessed.

The paper is divided into three distinct sections. In §2, I discuss swing-amplified noise in global simulations, and show that the behaviour in the Mestel ($V = \text{const.}$) disc is very similar to that reported by Toomre (*e.g.* this conference) for simulations in the shearing sheet. However, other more realistic models display much larger amplitude structure and wave coherence than can be accounted for by swing-amplified noise alone.

At first sight, the instability caused by a groove in a disc, which is described in §3, is totally unrelated to the previous section. The vigorous instability provoked by such an apparently arbitrary feature leads to a large amplitude spiral pattern. I present a simplified local analytic treatment which yields a rough prediction for the eigenfrequency.

The third part of this story describes an experiment which suggests how the two previous sections might be related. The coherent waves discussed briefly in §4 appear to result from a *recurrent cycle* of groove instabilities.

2 More than particle noise

2.1 ZANG DISCS

The stability properties of the infinite Mestel (1963) disc are quite remarkable. The disc has the surface density

$$\Sigma(r) = \frac{qV_0^2}{2\pi Gr},$$

which gives an exactly flat rotation curve all the way from the axis of rotation. Here, V_0 is the orbital speed for circular motion at any radius r which arises from this mass distribution when $q = 1$. Though the surface density is singular at the centre, the mass within any radius is, of course, finite.

Zang (1976) examined the global stability properties of centrally cut-out, but otherwise full-mass, models having this density distribution and found, rather surprisingly, that the most persistently unstable modes occurred for $m = 1$. The $m = 2$ modes could be completely suppressed if the velocity dispersion were comparatively modest and the central cut-out not too abrupt (see also Toomre 1977). The central cut out he used took the form of a taper in angular momentum, J , of the distribution function: $T(J) = [1 + (r_0 V_0 / J)^n]^{-1}$, where r_0 is some scale radius and the index $n \lesssim 2$ for stability. It now seems clear that the instabilities Zang found in models with $n > 2$ were edge-related modes.

In largely unpublished subsequent work, referred to in Toomre (1981), Zang and Toomre extended the study to include discs for which $q < 1$, *i.e.* embedded within a halo that did not alter the shape of the rotation curve. They found that a half-mass disc model ($q = 0.5$) could be *completely stable* to all global modes, provided the central taper was not too abrupt ($n \leq 4$). The radial velocity dispersion in their stable model $\sigma_u = 0.2835V_0$ which gives $Q = 1.5$ for all $r \gg r_0$.

The absence of instabilities makes this model an ideal test-bed in which to study, in a global context, a variety of phenomena that have been studied in the (local) shearing sheet model. Indeed Toomre (1981) already gives a memorable illustration of swing-amplification that is far more eye-catching than any diagram produced in an analysis of the shearing sheet, even though it was first discovered in that context some fifteen years earlier (Goldreich & Lynden-Bell 1965, Julian & Toomre 1966, hereafter JT).

2.2 SWING-AMPLIFIED NOISE

I have therefore run a series of simulations of this model which illustrate swing-amplified particle noise in a global context. These experiments are the logical counterparts to Toomre's simulations in the local shearing sheet model (a preliminary report of which is given in this volume). These are essentially empirical measurements of polarisation in a disc of particles characterised by $Q = 1.5$. As quiet starts would obviously be inappropriate for such an investigation, the initial azimuthal coordinates were chosen randomly.

Unfortunately, it is necessary, for obvious computational reasons, to truncate the disc at some outer radius also. I have not yet succeeded in doing this without provoking at least a mild $m = 2$ instability at the outer edge. Though the simulations are not completely stable, therefore, the growth of the outer edge mode is slow enough that the behaviour for the first hundred dynamical times is almost completely consistent with swing-amplified particle noise, as can be seen from the following.

In order to measure the amplitude of density variations, I formed the summation

$$A(m, \gamma, t) = \frac{1}{N} \sum_{j=1}^N \exp[im(\theta_j + \tan \gamma \ln r_j)], \quad (1)$$

at intervals during the simulations. Here, N is the number of particles and (r_j, θ_j) are the coordinates of the j th particle at time t . The resulting complex coefficients

A are the logarithmic spiral transformation of the particle distribution and γ is the inclination angle of the spiral component to the radial direction (positive for trailing waves).

The top line of panels in Figure 1(a–c) shows the time-averaged value of $|A|$ as a function of $\tan\gamma$ for the $m = 2, 3$ & 4 components from three different experiments which span two decades in N . The time interval, in units of r_0/V_0 , chosen for the average was $t = 25$ to $t = 100$ in each case – a period after the polarisation is reasonably well developed over most of the disc and before the outer edge instability had reached any significant amplitude.

The leading/trailing bias is obvious in all these plots, and is largest for $m = 2$. The horizontal dot-dash lines indicate the expectation value of $|A| (= \sqrt{\pi/4N})$ for randomly distributed particles (Sellwood & Carlberg 1984). The measured amplitude on the far leading side is completely consistent with randomly distributed particles in all three experiments. The peaks on the trailing side are higher than the leading signal by an approximately equal factor in the $N = 20\text{K}$ and $N = 200\text{K}$ experiments, but noticeably less when $N = 2\text{K}$. Spiral amplitudes in the $N = 2\text{K}$ experiment are so large as to be clearly visible which probably limits the measured bias for two reasons: peak amplitudes may well be limited by non-linear effects, and the velocity dispersion rises very quickly – making the disc less responsive. [This simulation is illustrated in Sellwood (1986).]

Following Toomre, I have estimated the bias that should be observed using the JT apparatus and found excellent agreement for the $m = 3$ & 4 components – the $m = 2$ bias in these global experiments is slightly larger than predicted by this local theory (Sellwood, in preparation).

In conclusion, results from these three experiments of this very nearly stable disc are quite consistent with theoretical expectations of swing-amplified particle noise.

2.3 MORE REALISTIC MODELS

Measurements over a comparable time interval from a parallel series of experiments with the “Sc” model of a disc galaxy used by Sellwood & Carlberg (1984, hereafter SC) are shown in the bottom row of panels in Figure 1(d–e). These experiments are not quite as comparable as would be desirable – it was necessary to use a lower mass fraction in the disc (30%) in order to prevent a rapid bar instability at the centre, and the initial velocity dispersion was set so as $Q = 1$ only. These differences shift the peak response to $m = 3$ and make the discs more responsive, respectively.

Nevertheless, the behaviour differs from that in the Zang models by more than can be accounted for by these reasons alone. The most obvious two differences are that the amplitudes on the leading side in the larger N experiments are no longer consistent with randomly distributed particles and nowhere do the signals decrease as $1/\sqrt{N}$. Though the amplitudes in the 200K particle experiment (f) are lower than those in (e), they rise throughout this time interval (1 – 4 rotation periods at the half-mass radius), attaining values no different from those in the lower N experiments by the end. This behaviour is clearly inconsistent with the hypothesis that the non-axisymmetric structure in these more realistic models can be attributed to swing-amplified particle noise.

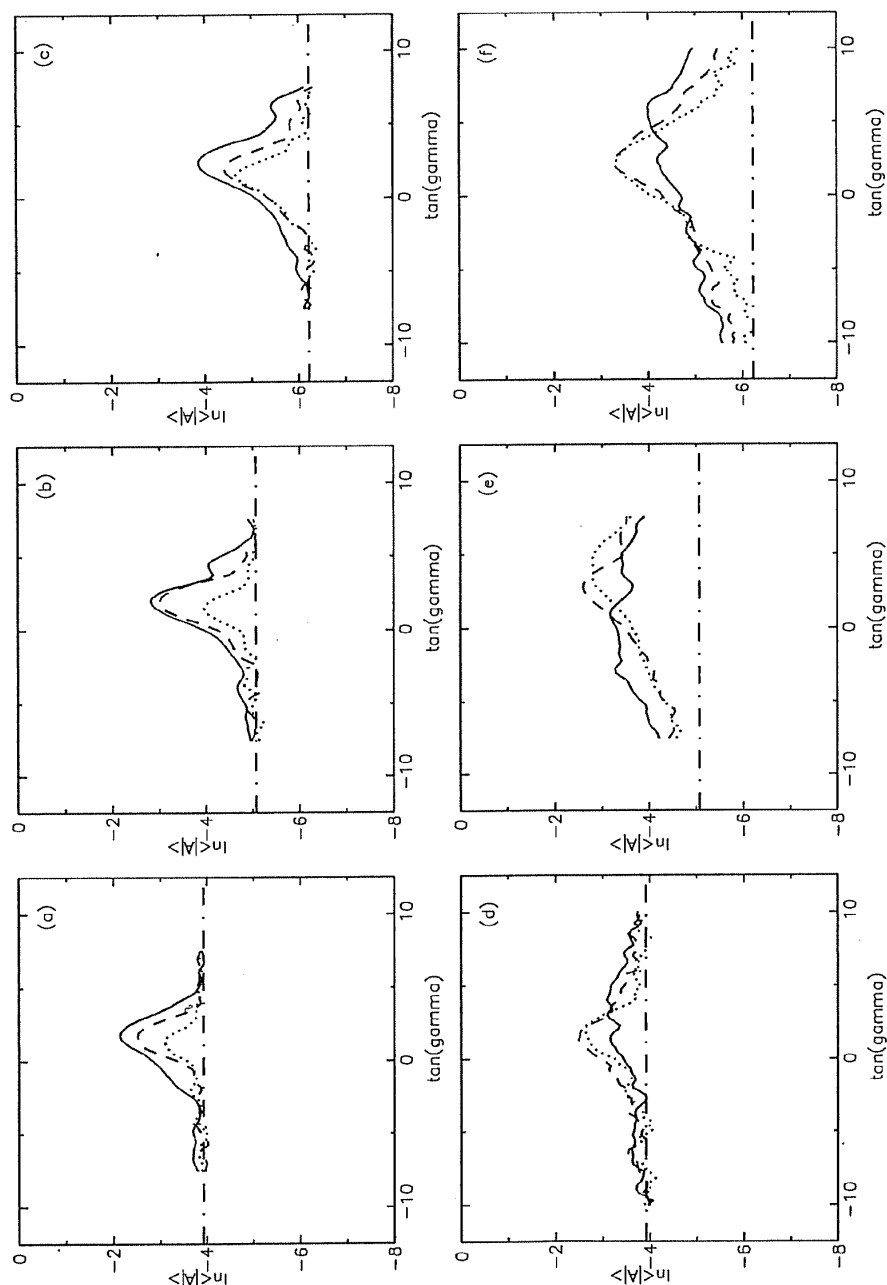


Figure 1 Time averaged values of the transform (equation 1) from two series of experiments in which the particle number is changed. The results for $m = 2$ – full drawn, $m = 3$ – dashed and $m = 4$ – dotted curves are shown in each case. The horizontal dot-dash line indicates the expectation value for N randomly distributed particles. The top row (a-c), show results from Zang models, the bottom row from Sc models, and N rises from 2K (left hand panels) through 20K (centre panels) to 200K (right hand panels).

2.4 COHERENT WAVES

As the amplitude of the spiral waves in these experiments always reached levels sufficient to heat the disc, the responsiveness and general level of activity declined as the experiments evolved. It was therefore impossible to study structure in these uncooled models over long periods. Therefore Carlberg and I, in further (unpublished) work with this mass model, devised a cooling algorithm which enabled us to run a long experiment that remained in a quasi-steady state.

Our cooling strategy in this case was to remove particles at random from the disc and to re-insert them at some other randomly chosen position on a locally-determined circular orbit. The distribution from which the new position was chosen was precisely that of the initial axisymmetric disc. We devised this cooling technique, which differs slightly from the accretion method used by SC, in order to avoid a steadily rising disc mass. This process might be thought of as mimicking the death of a star and the formation of a new star elsewhere in the disc – the gas phase of the disc simply being omitted from the dynamics. It is physically unrealistic in an additional important respect since it steadily redistributes angular momentum inwards, undoing that transferred outwards by the spirals, in order to maintain a quasi-steady distribution of angular momentum amongst the particles. The cooling rate we adopted was also quite unrealistically high – 15 particles per time-step, or 15% of the mass of the disc per rotation period.

We ran a $N = 20K$ model calculated according to this rule for 432 dynamical times (one rotation period at the half-mass radius is 16 dynamical times). Starting from an initial $Q = 1.7$, the model adjusted within the first ~ 30 dynamical times to quasi-steady values $1.8 \lesssim Q \lesssim 2.0$ over most of the disc. The $m = 3$ component of $|A|$, from equation (1), is contoured in Figure 2(a); the inclined stripes indicate recurrent shearing transient spiral waves, rather similar to those reported in SC. In this simulation, however, the amplitude of successive events soon settles to an approximately constant value, consistent with the quasi-steady state.

Figure 2(b) shows the power spectrum of this apparently stochastic sequence of spiral events. Narrow horizontal ridges in this diagram indicate coherent waves rotating at constant angular frequency over a wide range of inclination angles. The narrowness of the ridges in the frequency direction indicates that the individual waves must be very long lived – the ridges are scarcely broader than our frequency resolution.

The spatial shapes of six of these apparently coherent waves are shown in Figure 3. All are trailing spiral patterns which show remarkable respect for their principal resonances; the full-drawn circle marks the co-rotation resonance, the dotted circles the inner and outer Lindblad resonances (ILR and OLR respectively). All but the most rapidly rotating of these long-lived coherent waves possess ILRs, and only the slowest lacks an OLR within the particle distribution. The horizontal dashed lines in Figure 2(b) mark the limits of the angular frequency range for which waves have both Lindblad resonances within the disc of particles.

Though the waves survive for some time, they do not last indefinitely. Figure 2 shows data from the first half of the experiment – a similar analysis of the second half (not shown) reveals other long-lived waves, but their frequencies, while in the same range as those shown in Figure 2(b), are not identical. Each wave appears to have a finite lifetime, which unfortunately is not easy to measure – a reasonable estimate

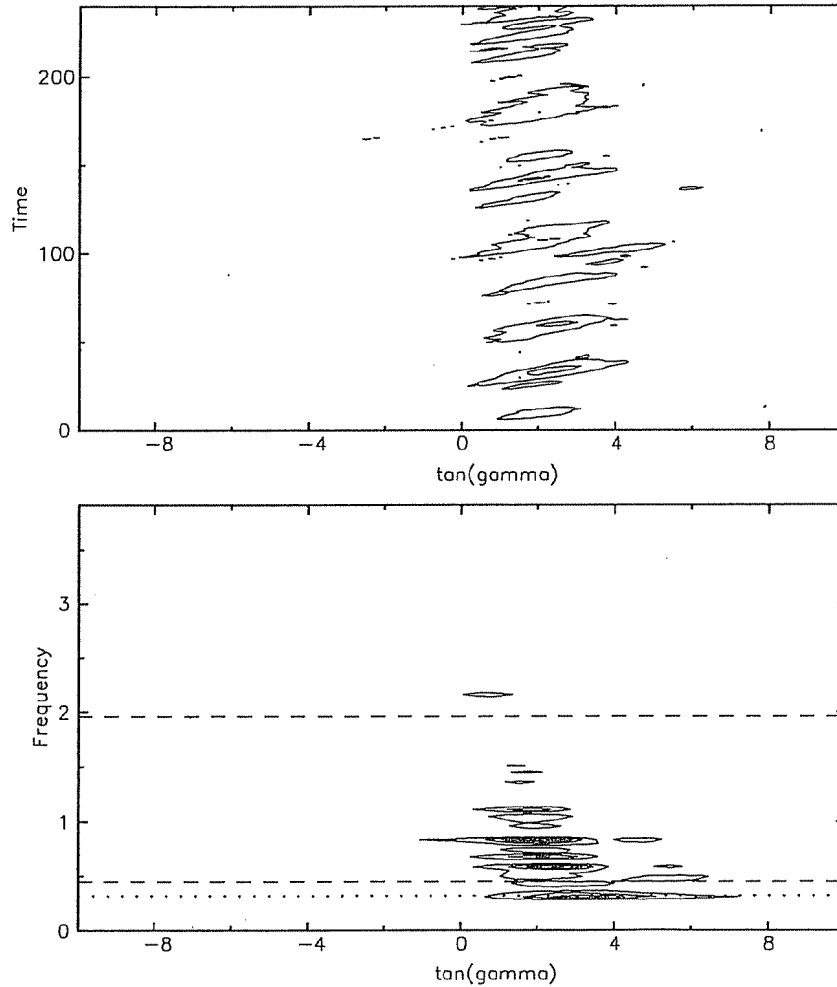


Figure 2 Results from a quasi-stationary Sc model. The rotation period at the half-mass radius in this model is 16 time units. (a) Contours of the $m = 3$ component of $|A|$ as a function of time and inclination angle. (b) A power spectrum of the same data, revealing a number of coherent waves at constant frequencies over wide ranges in pitch angles.

might be ~ 160 dynamical times or ten rotations. New waves continually appear to replenish those that decay.

Long-lived coherent waves are hardly to be expected from swing-amplified particle noise. It is tempting to describe them as modes of oscillation of the disc, though the fact that the majority possess ILRs is a real surprise. Orthodox spiral mode theory (*e.g.* Toomre 1981) might be able to account for (a) with a feed-back loop and (f) as an edge mode (the horizontal dotted line in Figure 3(b) shows the circular angular frequency at the outer edge) but it could not account for most of the frequencies we observe, because such waves should be strongly damped at both Lindblad resonances.

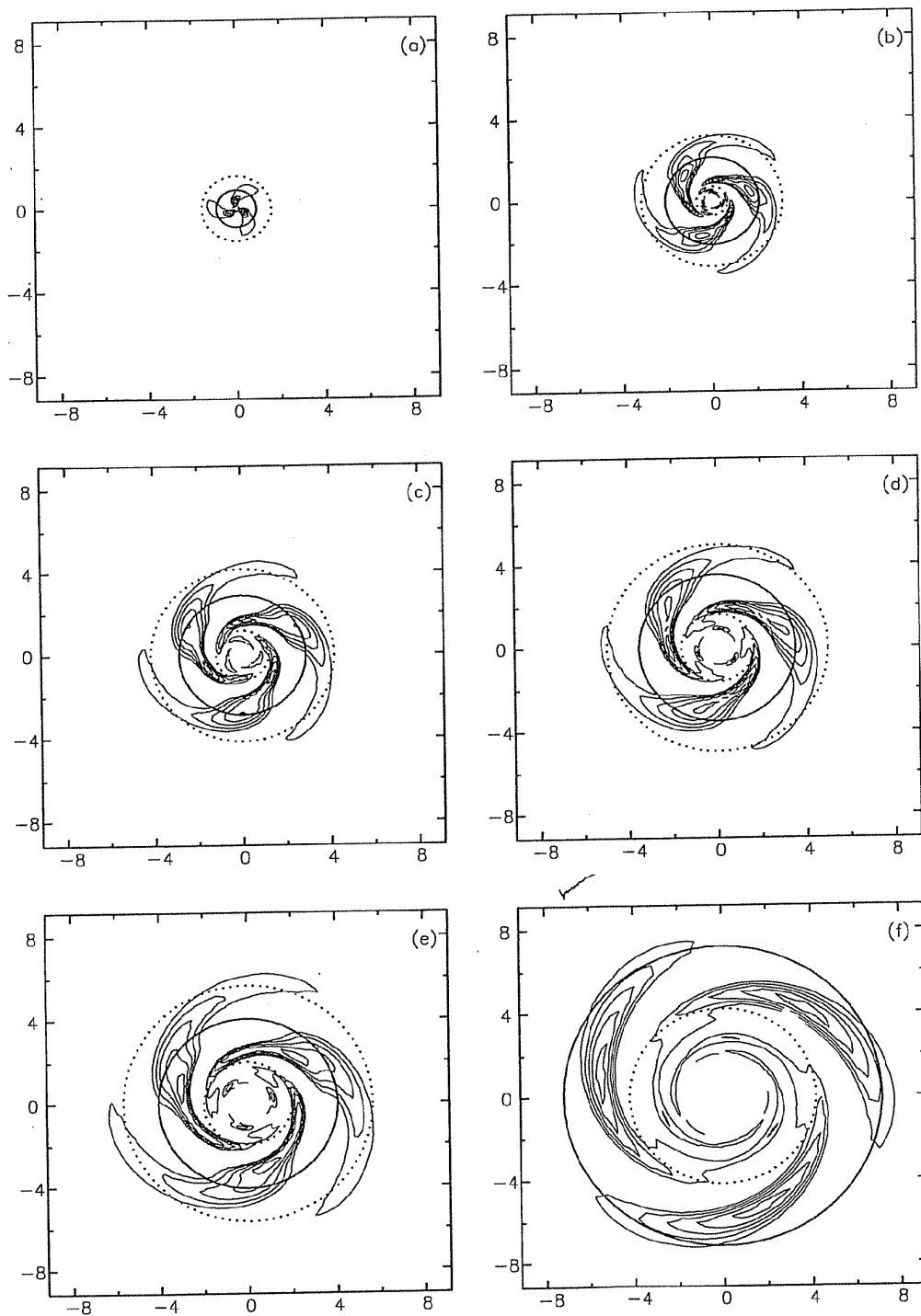


Figure 3 Six representative waves from the power spectrum in Figure 3(b). The co-rotation circle (full drawn) and the Lindblad resonances (dotted) are marked. The scales are in units of the scale radius of the Sc model (SC).

3 Groove modes

The instability described in this section arises when an otherwise smooth disc has a deficiency of particles over a narrow range of angular momenta. Further details are given in Sellwood & Kahn (1989). If the disc is cold, *i.e.* the radial velocity dispersion $\sigma_u = 0$, then such a disc has a narrow, axisymmetric groove in the surface density.

3.1 COLD DISC EXPERIMENTS

We use the half-mass Mestel disc, which is the mass distribution of the Zang disc described in §2.1, but we start all the particles on exactly circular orbits. We suppress axisymmetric instabilities by softening the inter-particle forces, preferring this approach to adding random motion only because the cause the instability can be directly observed (Figure 6) and the analysis (§3.2) is more easily related to the experiments. Discs with random motion should, and do, behave similarly. Moreover, the analysis remains valid for warm discs as long as the disturbance has a wavelength much longer than the mean epicycle size and one considers the distribution of guiding centres, instead of particles.

The surface density in our first experiment has no groove, and takes the form

$$\Sigma_0(r) = \frac{qV_0^2}{2\pi Gr}T(r), \quad \text{with} \quad T(r) = \begin{cases} [1 + (r/r_0)^4]^{-1} & \text{if } r < r_{\max}; \\ 0 & \text{otherwise.} \end{cases}$$

We set $q = 0.5$ (*i.e.* a half-mass disc) and $r_{\max} = 9r_0$. The minimum softening length required to suppress axisymmetric instabilities in a cold disc is $\epsilon_{\min} = \lambda_{\text{crit}}/2\pi e$, where e is the base of natural logarithms. We adopt a softening length of $1.5\epsilon_{\min} \simeq 0.138r$, *i.e.* increasing linearly with radius.

We augment the central attraction of the model by an amount sufficient to ensure centrifugal balance when all particles orbit at speed V_0 . This central force, which can be thought of as arising from a halo, also corrects the forces from the particle distribution for the central taper, outer cut-off and softening. The particles are smoothly distributed at the outset (*i.e.* a quiet start) and we restrict the disturbance forces to those arising from the $m = 2$ component of the surface density only, enabling us to confine the particles to a semi-circle. Again this restriction, which makes no difference to the behaviour in the linear regime, is not a requirement of the computation. It does, however, further simplify the observed behaviour and considerably reduces the number of particles we need employ.

We adopt a system of units such that $r_0 = V_0 = G = 1$. The orbital period at $r = 1$ is therefore 2π dynamical times.

A simulation using just 15K particles was run for 200 dynamical times during which period no visible change occurred. Fourier analysis revealed a very slowly growing outer edge instability, but which was still well below its saturation amplitude by the end of the test run. We conclude therefore that the basic cold disc model is stable enough to global $m = 2$ perturbations for our purposes.

The next experiment we describe had almost the same initial particle distribution, but differed by having a narrow, axisymmetric groove in the surface density of the Lorentzian form

$$\Sigma(r) = \Sigma_0(r) \left[1 - \frac{\beta w^2}{(r - r_*)^2 + w^2} \right], \quad (2)$$

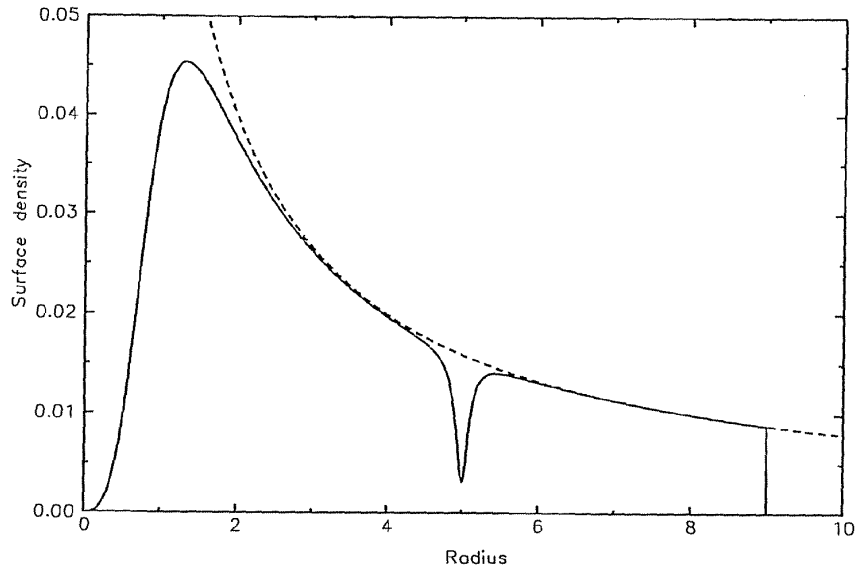


Figure 4 The axisymmetric surface density distribution in the model illustrated in Figure 5 (full drawn curve). The dashed curve shows the basic Mestel disc without an inner taper, groove or outer edge. Units are in r_0 and $V_0^2/(Gr_0)$.

as illustrated in Figure 4. We set the groove centre $r_* = 5$, its width $w = 0.1$ and fractional depth $\beta = 0.8$. Results from this simulation are shown in Figure 5 – the model is drastically unstable and develops a global, large-amplitude, spiral pattern.

The early evolution of the model is omitted from Figure 5 because no visible changes occur, but Fourier analysis can detect a rapidly growing instability from a very early stage. The Fourier coefficients are extremely well fitted by a single exponentially growing mode having the spatial form shown in Figure 6 and eigenfrequency $\omega = 0.383 + 0.072i$. The growth rate, $\Im(\omega)$, is therefore more than one third the pattern speed, $\Re(\omega)/m$, indicative of an extremely vigorous dynamical instability.

Figure 6 shows that co-rotation (the full drawn circle) is close to, but just outside the groove centre (marked by a dashed circle), and that the disturbance is very strongly localised in this region. There are weaker, trailing spiral arms extending towards the Lindblad resonances (dotted circles) on either side of the groove.

3.2 LOCAL ANALYTIC TREATMENT

The global instability is driven by the non-axisymmetric density changes that develop in a narrow range of radii around the groove. We therefore find that a local analysis of that region yields reasonable estimates of the mode frequency.

We use co-ordinates (ξ, η) to represent the forced radial and transverse displacements of a guiding centre from its circular orbit caused by the presence of wave-like disturbance potential. The origin of these displacement co-ordinates moves on a circular path at radius r with orbit speed V_0 and therefore angular velocity $\Omega(r) \equiv V_0/r$.

We consider a weak, uniformly rotating perturbing gravitational field with a potential of the form $\Phi(r)e^{i(m\theta - \omega t)}$, which is small enough for a linearised treatment of

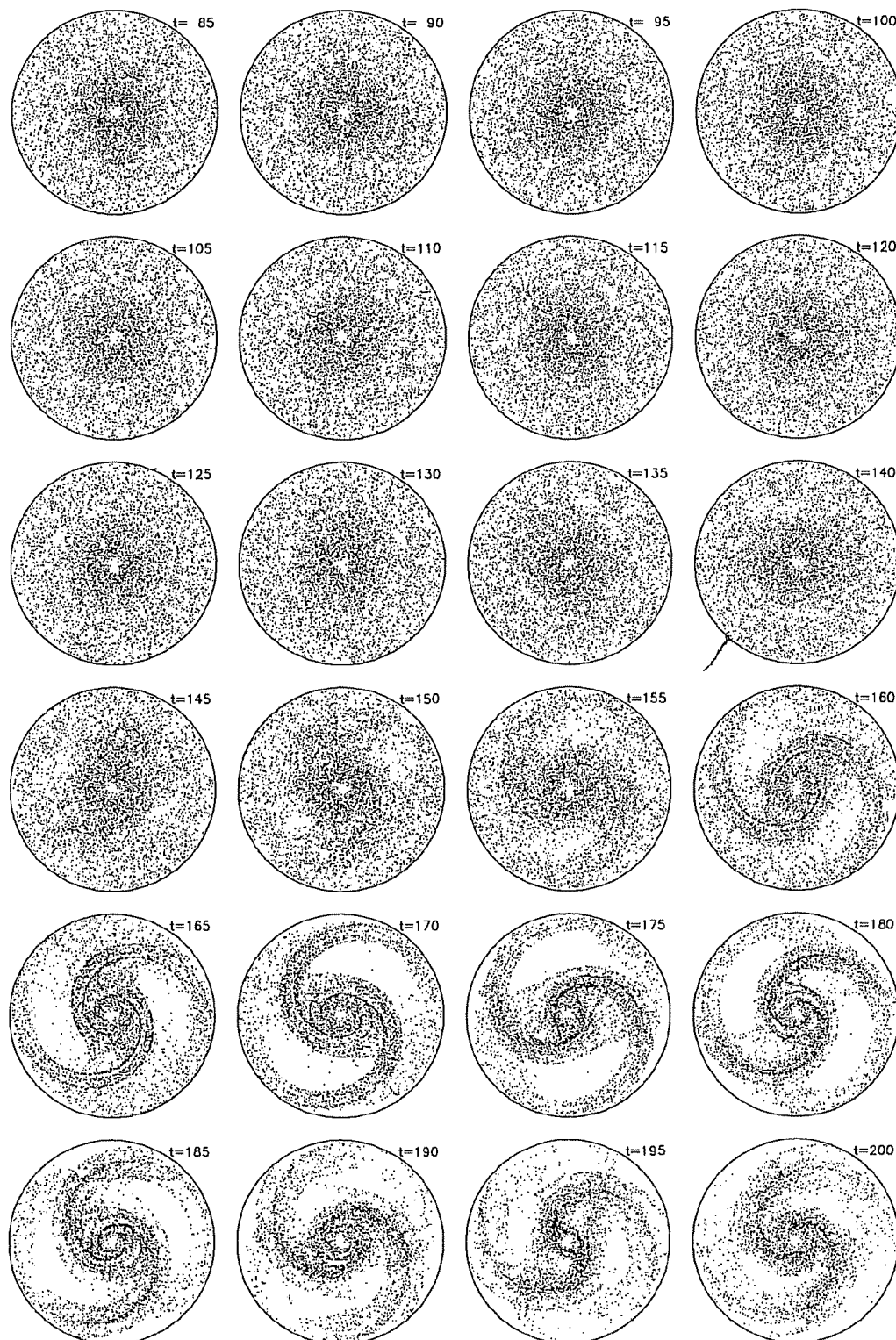


Figure 5 Evolution of a cold disc model with a deep, narrow groove. Times are in units of r_0/V_0 – a rotation period at the groove is therefore 10π . Note that the early evolution of the model, during which no visible changes occur, is omitted. The calculation was restricted so that only $m = 2$ components of the disturbance potential affected the motion of the particles.

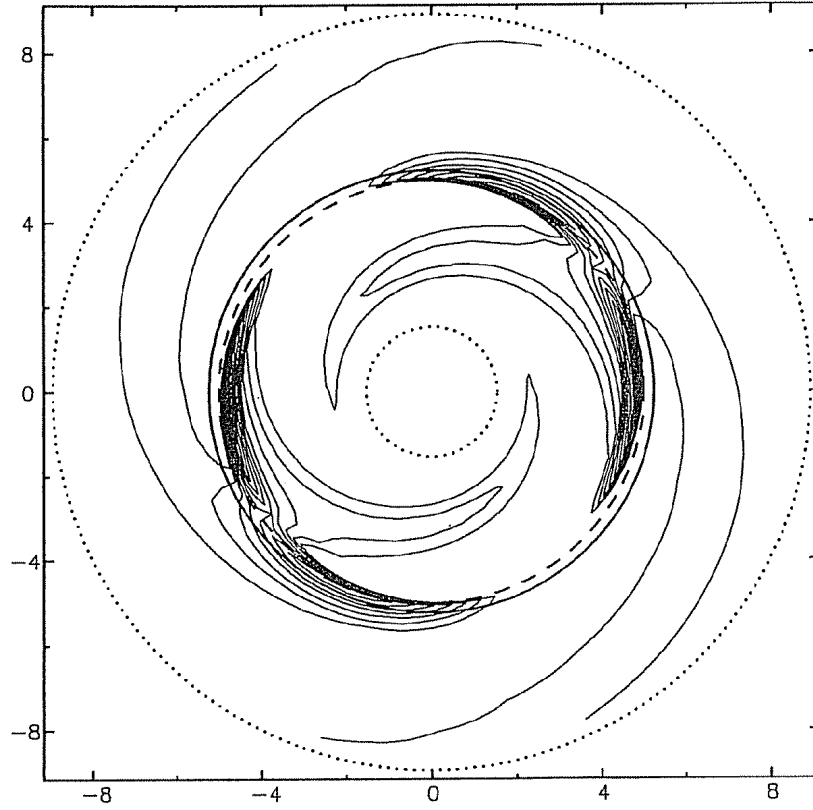


Figure 6 The best fit exponentially growing mode to the small amplitude evolution of the model shown in Figure 5. Only the positive part is shown. The full drawn circle marks co-rotation and the dotted circles the Lindblad resonances for the best-fit frequency. The groove centre is marked by the dashed circle.

the forced motions to be valid.

The linearised equations of motion are

$$\begin{aligned}\ddot{\xi} + 2r\Omega\Omega'\dot{\xi} - 2\Omega\dot{\eta} &= \frac{\partial\Phi}{\partial r} \\ \ddot{\eta} + 2\Omega\dot{\xi} &= \frac{im\Phi}{r},\end{aligned}$$

with the exponential factor understood. We have used a dot to denote differentiation with respect to time (following the path of the guiding centre) and a dash denotes differentiation with respect to r . These equations can be readily integrated; setting $\kappa^2 = 2\Omega^2$ (for a flat rotation curve) we obtain

$$\xi \sim -\frac{m}{V_0\kappa\nu}\Phi \quad \text{and} \quad \eta \sim \frac{im}{r\kappa^2\nu^2}\Phi, \quad (3)$$

where $\nu = (\omega - m\Omega)/\kappa$, a dimensionless forcing frequency that has a small real part near co-rotation. We have therefore neglected terms containing $\partial\Phi/\partial r$, since these enter with lower power of ν in the denominator and are considerably smaller than the terms we retain.

The equation of continuity relates the disturbance surface density, Σ_1 , to the displacements of the guiding centres; *viz.*

$$\Sigma_1 = -\frac{1}{r} \frac{\partial}{\partial r}(\Sigma r \xi) - \frac{im}{r} \Sigma \eta.$$

In our current local treatment, in which r is assumed large, we can neglect curvature and use the approximate relation

$$\Sigma_1 \simeq -\frac{\partial}{\partial r}(\Sigma \xi) - \frac{im}{r} \Sigma \eta.$$

We substitute from equations (3), and neglect radial derivatives of κ and Φ , which vary slowly across the narrow region around co-rotation; *i.e.* the dominant radial derivatives are those of Σ (which has a narrow feature in the radial range of interest) and $1/\nu$ (which varies rapidly because ν is small). In this approximation, two of the terms cancel and we are left with

$$\Sigma_1 \sim \Sigma' \frac{m}{V_0 \kappa \nu} \Phi. \quad (4)$$

Equation (4) clearly gives a surface density of the form observed for the mode (Figure 6). The disturbed density is large where Σ' is large, but the opposite signs of this gradient on each side of the groove cause a phase shift of almost π (*i.e.* a 90° shift in real space) across the groove.

Since we have neglected curvature, symmetry demands that co-rotation should be at the centre of the groove, which determines the real part of the eigenfrequency. We now estimate the growth rate, ω_i .

Because our softening length is large compared with the width of the groove, we may compute the potential of the entire disturbance as if it were a single sinusoidal wave on the circle at $r = r_*$ having an amplitude

$$C = \int \Sigma_1 dr \simeq \int \Sigma' \frac{m}{V_0 \kappa \nu} \Phi dr, \quad (5)$$

where the range of integration includes all stars whose orbits are substantially perturbed.

We can write the surface density (2) in the vicinity of the groove in the form

$$\Sigma(x) = \Sigma_0(r) \left[1 - \frac{\beta w^2}{(r - r_*)^2 + w^2} \right] \equiv \frac{\Sigma_0(r)}{2} \left[2 + i\beta w \left(\frac{1}{x - iw} - \frac{1}{x + iw} \right) \right],$$

where $x = r - r_*$. Using this in (5), we find

$$C = \frac{m}{V_0} \Phi \int_{-\infty}^{\infty} \frac{-i\beta w \Sigma_0}{2} \left[\frac{1}{(x - iw)^2} - \frac{1}{(x + iw)^2} \right] \frac{1}{\omega - m\Omega} dx.$$

Writing $\omega - m\Omega = mV_0(x - \lambda)/r_*^2$, where $\lambda = r_*(1 - \omega r_*/mV_0)$, we may evaluate the integral by closing off the contour in the lower half of the complex plane (since $\Im(\lambda) < 0$), and obtain

$$C = \frac{m\Phi}{V_0} \cdot \frac{-i\beta w \Sigma_0 r_*^2}{2mV_0} \cdot \frac{-2\pi i}{(\lambda - iw)^2}.$$

Because co-rotation is at r_* , $\lambda = -i\omega_i r_*^2/mV_0$ (*i.e.* purely imaginary). The above expression therefore simplifies to

$$C = \frac{\pi m^2 \beta w \Sigma_0 r_*^2 \Phi}{(\omega_i r_*^2 + mV_0 w)^2}. \quad (6)$$

The potential in the groove arising from this sinusoidally varying disturbance with mass per unit length C is

$$\Phi = 2GC K_0 \left(\frac{m\epsilon}{r_*} \right),$$

where K_0 is the Bessel function of imaginary argument and ϵ is the softening length. Substituting this into (6), and setting $\Sigma_0 = qV_0^2/2\pi Gr$, we obtain the desired expression for the growth-rate of the mode

$$\omega_i = \frac{mV_0 w}{r_*^2} \left\{ \left[\frac{q\beta r_*}{w} K_0 \left(\frac{m\epsilon}{r_*} \right) \right]^{1/2} - 1 \right\}. \quad (7)$$

This expression indicates that we expect instability only for grooves in which the fractional depth

$$\beta > \frac{1}{qK_0} \frac{w}{r_*}, \quad (8)$$

i.e. not for infinitesimally shallow grooves. The critical depth is very small, however; *e.g.* in our experiments, $q = 0.5$, $w = 0.02r_*$ and $K_0 \simeq 1.45$ (for $m = 2$), so we should expect an instability whenever the fractional depth exceeds merely 2.8%! Notice also that the critical depth required increases with the groove width (though our analysis assumes this to be small); it would seem therefore, that the instability requires a critical density *gradient* on the sides of the groove.

We may compare the predictions of this local theory with the empirical results from our experiments. The eigenfrequency expected is $\omega_r = 0.4$ (for co-rotation at the groove centre) and $\omega_i = 0.035$ [from (7)]. That observed in the simulation is $\omega = 0.383 + 0.072i$. The real parts are in reasonable agreement, but our prediction considerably underestimates the observed growth rate. Two approximations in our analysis are largely responsible for this poor agreement, the principal being the additional contribution to Φ which comes from the supporting response of the disc. Our neglect of curvature appears to be of lesser importance; in other experiments, in which we raised the azimuthal mode number to $m = 3$ and 4, where it is more justifiable to neglect curvature, predictions for the growth rate from equation (7) are somewhat closer to the observed values (and co-rotation approaches the groove centre more closely still).

But most of the growth rate discrepancy is removed only in an improved treatment which includes the supporting response from the background disc (Sellwood & Kahn 1989). The spiral response of the disc on either side of the groove can be thought of as the polarisation response, or wake, induced by the growing non-axisymmetric disturbance in the groove. Discussions of wakes usually focus on the steady response to a large co-orbiting disturbing mass (*e.g.* JT); in this case, we have an exponentially growing disturbance that induces an exponentially growing response.

The instability produces a growing sinusoidal distortion to each side of the groove, and we must expect it to saturate once the distortions exceed the groove width, *i.e.* when further perturbations to the orbits of particles no longer produce corresponding increases in disturbance forces. At this stage, the mass distribution at the radius of the original groove has large non-axisymmetric variations – to a good approximation, it will consist of two blobs (for the $m = 2$ component). These large amplitude blobs will dissolve only slowly and each will continue to induce a spiral wake for some considerable time after the mode has saturated, as can be seen in Figure 5.

As the clearest possible example of how untested theory can be completely misleading, I note that the analysis provided here implies that a ridge, rather than a groove, would not provoke instabilities. As a ridge would be characterised by a negative value for β , equation (8) indicates that no instability should be expected. A simple experimental test of this prediction showed that it was completely wrong! A ridge provokes instabilities just as fierce as those from a groove. We were able to understand ridge modes only when we extended the analytic treatment presented here to consider wave-like perturbations travelling around the ridge. This more sophisticated treatment is presented in Sellwood & Kahn (1989)

4 A recurrent instability cycle

In this section I argue that an experiment from my recent collaboration with D. N. C. Lin provides a connecting link between the two previous sections. Our project was begun in the hope that N -body simulations of low mass particle discs around a central point mass might reveal non-axisymmetric instabilities of relevance to accretion discs. The experiments did reveal non-axisymmetric instabilities, but which are, however, likely to be of much greater significance to spiral structure in galaxies than to instabilities in accretion discs!

The simulation, which is discussed in detail elsewhere (Sellwood & Lin 1989), revealed a recurrent instability cycle of the following form: An instability somewhere in the disc causes a non-axisymmetric wave to grow to large amplitude. Particles at the Lindblad resonances of the wave are strongly scattered and change their angular momenta. As the resonances are narrow, the distribution function is severely depleted over a narrow range of angular momentum, which leads to a new groove-type instability with co-rotation at the radius of the Lindblad resonance of the previous wave.

Figure 7 shows how the distribution function changed in the experiment between the start and a moment 267 dynamical times later. The particle distribution is shown in action space: the abscissa of each is its angular momentum and the ordinate its radial action. (Particles on more eccentric orbits have larger radial actions.) The arrows point to the principal resonances (co-rotation, inner and outer Lindblad resonances) for the five waves observed in the experiment up to the moment illustrated. The resonant scattering that has occurred has produced substantial heating (the particles have much larger radial actions) and the distribution function is also much less smooth than at the start. Each tongue of particles reaching to large radial action was produced by scattering at a Lindblad resonance.

But the most interesting aspect of this revealing diagram is that the most recent wave has left a clear deficiency of particles having angular momenta ~ 1.35 . This

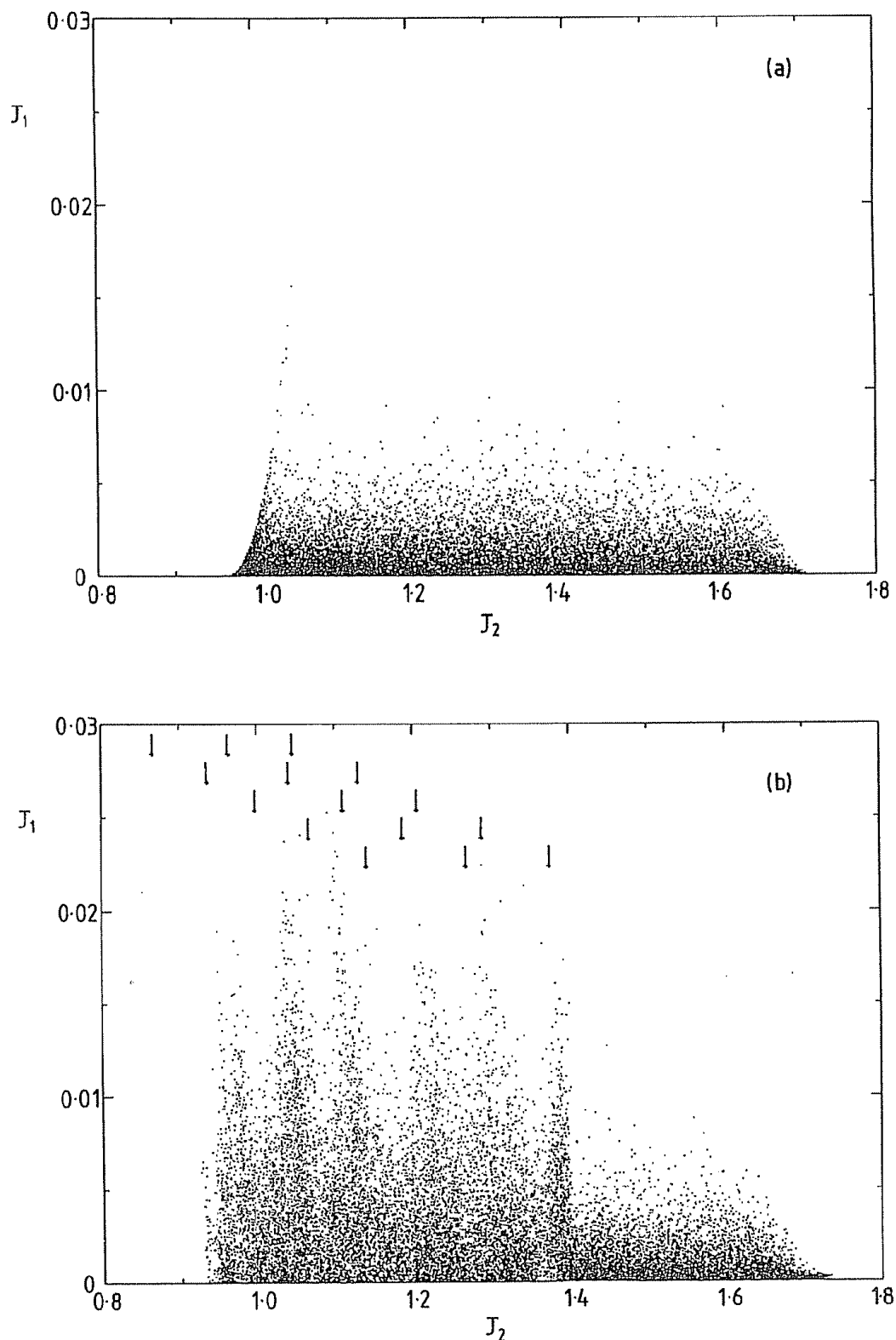


Figure 7 The phase space distribution of particles in the experiment described in Sellwood & Lin (1989) (a) Shows the situation at the start and (b) after 267 dynamical times. The spread in J_2 (angular momentum) reflects the radial extent of the annulus and those particles with large J_1 (radial action) are on more eccentric orbits. Only one fifth of the 100K particles used in the simulation are plotted in each panel. The arrows in (b) point to the locations of co-rotation and the two Lindblad resonances for the five waves observed in the model by time 267.

deficiency drives a new instability in the disc which begins its linear growth at about the time illustrated. The new instability is quite clearly a groove-type mode – co-rotation lies at precisely the angular momentum of the deficiency in the distribution function. Note that in this case we have a “groove” in the distribution of guiding centres; because particles have random motion, there is no noticeable groove in the surface density of the disc.

5 Discussion

In this paper I have collected the evidence indicating that the recurrent transient spirals seen in many simulations results from spiral *modes* that grow rapidly and decay only to be replaced by new instabilities. This picture is radically different from two other current views of spiral structure. Bertin *et al.* (1989, and references therein) argue that spiral patterns result from mild instabilities which lead to quasi-steady waves once non-linear effects in the gas are taken into account. It is not at all clear that the models they propose could avoid the far more vigorous recurrent cycle of groove modes presented here. Toomre, on the other hand, stresses the role of local spiral “streaks” resulting from density fluctuations in the disc (*e.g.* this conference). Though these undoubtedly occur, it is far from clear that real galaxy discs are “lumpy” enough for strong spirals to be produced in this way.

The original evidence for something more than noise came from the experiments of SC. The discussion of §2 bolsters that case considerably by contrasting the Sc models with the almost perfect illustration of swing-amplified particle noise manifested by the Zang discs – spiral amplitudes in the more realistic Sc disc hardly changed with N . Moreover, the recurring transient patterns in cooled Sc models resulted from the super-position of a few long-lived coherent waves. Most of these waves, which could be picked out by Fourier analysis, had two Lindblad resonances within the disc and therefore could not be accounted for by orthodox mode theory.

In the two subsequent sections I demonstrate that a groove-like feature in the angular momentum distribution provokes a fierce instability and show how modes of this type can recur in an instability cycle. Resonant scattering by a large amplitude wave, created by the saturation of one mode, carves a groove that precipitates a new linear instability. As the instability cycle also heats the disc, making it less susceptible to further instabilities, activity must fade after comparatively few cycles unless the disc is cooled. The presence of a dynamically significant fraction of gas in the galaxy is therefore essential if the galaxy is to continue to display spiral structure over a long period.

Though the connection still needs to be demonstrated in massive discs, this recurrent groove mode cycle seems at last to offer an explanation for the very intriguing spiral activity that had been observed in simulations for many years. Experiments are currently in hand to attempt to substantiate this claim.

This paper has also brought out the importance of relating results from simulations to the theory, and *vice-versa*. Only through the quantitative comparison of the results from the Zang model experiments with the predictions of swing-amplified particle noise, could the more vigorous structure in the Sc models be clearly identified as something more than noise. On the other hand, theory, unfettered by cross checks

with experimental results, can easily go astray. An excellent example is provided by the beautifully straightforward linear analysis, which gives a reasonable description of groove modes, but which incorrectly predicts that axisymmetric density ridges in a disc are not destabilising!

Much of the work reported in §2 was done in collaboration with Ray Carlberg and has yet to be published. Franz Kahn was my collaborator for work described in §3. The author acknowledges the support of an SERC Advanced Fellowship.

References

- Bertin, G., Lin, C. C., Lowe, S. A. & Thurstans, R. P., 1989. *Astrophys. J.*, **338**, pp. 78 & 104.
- Goldreich, P. & Lynden-Bell, D., 1965. *Mon. Not. R. Astron. Soc.*, **130**, 124.
- Julian, W. H. & Toomre, A., 1966. *Astrophys. J.*, **146**, 810 (JT).
- Mestel, L., 1963. *Mon. Not. R. Astron. Soc.*, **126**, 553.
- Sellwood, J. A., 1986. In *The Use of Supercomputers in Stellar Dynamics*, Lecture Notes in Physics **267**, p. 5, eds. Hut, P. & McMillan, S., Springer-Verlag, New York.
- Sellwood, J. A., 1989. In *Nonlinear Phenomena in Vlasov Plasmas*, p. 87, ed. Doveil, F., Éditions de Physique, Orsay.
- Sellwood, J. A. & Carlberg, R. G., 1984. *Astrophys. J.*, **282**, 61 (SC).
- Sellwood, J. A. & Lin, D. N. C., 1989. *Mon. Not. R. Astron. Soc.*, in press.
- Sellwood, J. A. & Kahn, F. D., 1989. *Mon. Not. R. Astron. Soc.*, in preparation.
- Toomre, A., 1977. *Annu. Rev. Astron. Astrophys.*, **15**, 437.
- Toomre, A., 1981. In *Structure and Evolution of Normal Galaxies*, p. 111, eds. Fall, S. M. & Lynden-Bell, D., Cambridge University Press: Cambridge.
- Zang, T. A., 1976. *PhD thesis*, MIT.